coatings

MDPI

Article

Archaeometric Investigations of the Chalcolithic Pottery from Topolița—Neamț County, Romania

Rodica-Mariana Ion [1,2,*], Vasile Diaconu [3], Gabriel Vasilievici [1,*], Lorena Iancu [1], Ramona Marina Grigorescu [1], Luiza-Andreea Mîrț [1], Elvira Alexandrescu [1], Anca Irina Gheboianu [4] and Sofia Slamnoiu-Teodorescu [4]

1 National Institute for Research & Development in Chemistry and Petrochemistry—ICECHIM, Research Group 'Evaluation and Conservation of Cultural Heritage', 202 Splaiul Independentei, 060021 Bucharest, Romania
2 Doctoral School of Materials Engineering Department, "Valahia" University of Targoviste, 35 Lt. Stancu Ion, 130105 Targoviste, Romania
3 Museum of History and Ethnography Târgu Neamț/Neamț County Museum Complex, 37 Ștefan cel Mare St., 615200 Târgu Neamt, Romania
4 Institute of Multidisciplinary Research for Science and Technology, Valahia University of Targoviste, 130004 Targoviste, Romania
* Correspondence: rodica.ion@valahia.ro (R.-M.I.); gvasilievici@icechim.ro (G.V.)

Abstract: The current work deals with specific investigations on the ceramic fragment samples from the archaeological site of Topolița (Eastern Romania), which is essentially unexplored to date. X-ray diffraction (XRD) has shown that the ceramics contain quartz, berlinite, mica (muscovite), calcite, and opaque minerals, such as hematite. All evidence indicates the use of raw materials with a low limestone content (poor Ca clays) for the manufacture of these ceramics (Ca < 3.6%). The wavelength dispersive X-ray fluorescence (WDXRF) measurements indicated the presence of Al, Si, Fe, Ca, Zn, P, and K. All these data are well correlated with energy dispersive spectroscopy (EDS), which is used as an additional technique of scanning electron microscopy (SEM). Through thermogravimetry and porosimetry, some information have been obtained, with the results being correlated with the chromatic parameters that characterize the samples after burning: Various shades of color (red color with sparkles and partially or totally black interior), differently colored engobes, white pigment encrusted with white color from calcite, gypsum, clays, and quartz, as well as carbon deposits in the pores of the pottery, all specific to the Chalcolithic ceramics from this region. The recorded FTIR spectra of these samples led to the identification of calcite, quartz, gypsum, and aluminum phosphate, present as berlinite in all the pottery specific to this area. In addition, the presence/absence and the amount of specific chemical elements in the white pigments (e.g., calcium, aluminum, phosphorus, silicon, sulfur) could be used as indicative for the identified mineral compounds (XRD and FTIR). Calcite and silica-rich sediments as the primary decoration pigments, have been identified in this case.

Keywords: archaeometry; Precucuteni; berlinite

check for updates

Citation: Ion, R.-M.; Diaconu, V.; Vasilievici, G.; Iancu, L.; Grigorescu, R.M.; Mîrț, L.-A.; Alexandrescu, E.; Gheboianu, A.I.; Slamnoiu-Teodorescu, S. Archaeometric Investigations of the Chalcolithic Pottery from Topolița—Neamț County, Romania. *Coatings* **2023**, *13*, 488. https://doi.org/10.3390/coatings13030488

Academic Editor: Sandra Dirè

Received: 30 December 2022
Revised: 12 February 2023
Accepted: 20 February 2023
Published: 22 February 2023

Copyright: © 2023 by the authors. Licensee MDPI, Basel, Switzerland. This article is an open access article distributed under the terms and conditions of the Creative Commons Attribution (CC BY) license (https://creativecommons.org/licenses/by/4.0/).

1. Introduction

The studies carried out on ceramics occupy an important place in archaeological records, with valuable information on the social, economic, and symbolic aspects specific to the Chalcolithic period in South-East Europe. One of the most debated topics in the analysis of European prehistory is the Cucuteni civilization (5th–4th millennia BC), which expanded on the eastern part of Romania [1].

The archaeological site of Topolița (with identified signs of civilization), is located in the Subcarpathian area of Moldavia (Eastern Romania), in the northeastern part of Neamț County, in the central area of the depression with the same name. The multilayers

settlement is located approximately 6 km south of Târgu Neamț city and occupies a part of the low terrace to the right of the Valea Seacă stream, an affluent of the Topolița river [2].

Considering the fact that the site is multilayered, in 2017, a geophysical scan was carried out by a German team from the University of Erlangen-Nürnberg. On that occasion, the traces of several residential structures (25), somewhat unevenly arranged on an area of approximately 2 ha, were identified [3]. Since the results of the non-invasive investigations were very promising, in 2019, a systematic archaeological research began in this settlement [4].

From a chronological and cultural point of view, several stages of attendance were documented within the site: Neolithic (Linear Pottery culture), Eneolithic (Precucuteni culture, middle phase), Late Bronze Age (Noua culture), Iron Age (culture Poienești-Lucașeuka), and Late Antiquity (IV century AD, Sântana de Mureș culture). The most consistent vestiges belong to the early Eneolithic (second half of the 5th millennium BC). To date, five dwellings of the Precucuteni culture have been studied, as well as some household pits from the same period.

The Topolița site is important since in the geographical space where it is located—the Neamț Depression—few settlements of the Precucuteni culture are known. Through this research, regarding the specificity of the Eneolithic communities in the submontane area, a series of very valuable scientific information have been obtained.

The establishment of the Precucuteni culture community in this place was conditioned by the existence of a space favorable to agriculture, a fact proven not only by thorough pedological analyses [5], but also by the existence of important salt sources located at a distance of 6–8 km.

The most important amount of archaeological remains specific to the Eneolithic habitation is represented by pottery, technologically divided into two main categories, coarse and fine, as well as decorated with applied, printed, and incised decorations. Since currently there are only few data related to the technology of ceramic production from the Precucuteni culture, we proposed an archaeometric analysis on a sample of vessel fragments. Although it is known that during this period painting was rarely used to decorate clay containers, the presence of pigments on some ceramic fragments required their study. To date, no physical-chemical analyses have been published on the pigments used in the Precucuteni culture environment.

The samples from the archaeological site Topolița belong to the Precucuteni culture, and thus to the ancestors of the famous Cucuteni culture.

To date, several studies have been published in the specialized literature on ceramic samples, studies that have contributed to the elucidation of aspects related to the composition, structure, and dating of these samples, as well as their temporal and geographical location [6,7]. The structure of the investigated artifacts, chemical composition, as well as morphology and surface topography were determined using different investigation techniques [8,9]. Analytical methods, such as X-ray diffraction (XRD) and wavelength-dispersive X-ray fluorescence (WDXRF) are used to determine the oxide composition present in artifacts. Moreover, optical microscopy (OM), stereomicroscopy, scanning electron microscopy (SEM), Raman spectroscopy or Fourier transform infrared spectroscopy (FTIR) are used to identify the porous, mineral, and amorphous phases, texture and orientation of grains, and the aggregates present in ceramic samples [10]. Furthermore, thermogravimetry or thermogravimetric analysis (TGA) serves to analyze the thermal behavior of the investigated samples.

In this paper, for the first time in the literature, some archaeometric methods will be used on some samples of ceramic fragments from the archaeological site of Topolița (Eastern Romania). For the investigated samples, the chemical composition, the morphology and topography of the pottery, elementary and molecular information for contained pigments, and their deterioration processes, will be investigated and discussed. Moreover, the firing temperature and firing atmosphere will be estimated.

2. Materials and Methods

2.1. Materials

The place where the sample has been collected is located in the North-Eastern part of Romania, as presented in Figure 1.



Figure 1. The site from Topolița: (**1**) Dwelling no. 4; (**2**) pedological sequence; (**3**,**5**) pottery; (**4**) anthropomorphic figurines.

Ten pottery samples, representative for the Precucuteni civilization, have been selected for the present study. The pottery samples were cleaned with distilled water in an ultrasonic bat. Then, small slices have been cut across the ceramic wall for analytical investigations. All the samples show voids or gaps, cracks, scratches on the surfaces, internal degradation tracks, which are necessary for investigation. The visual aspects (photos), optical microscopy, and stereomicroscopy images of the studied samples are presented in Table 1.

Table 1. The sample labeling: Codification, photos, optical and zoom microscopy images of the studied pottery fragments.

No. of Sample	Visual Aspect	Optical Microscopy	Stereomicroscopy
1A		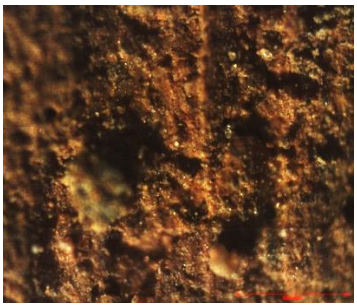	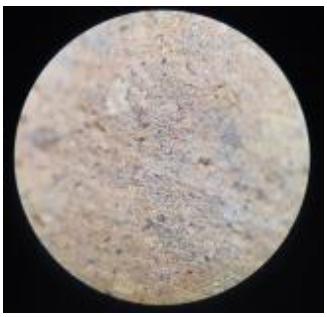
1B		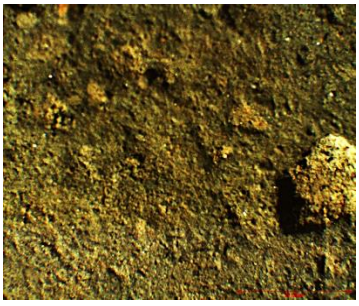	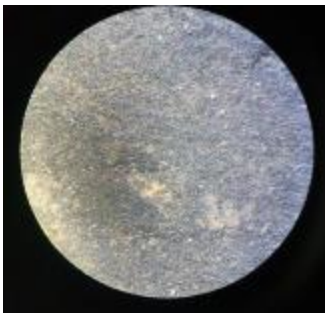
1C		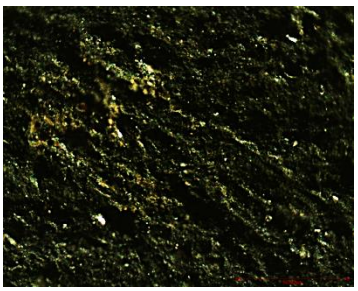	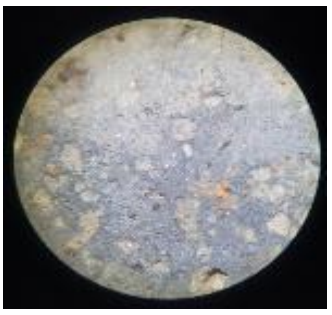
2			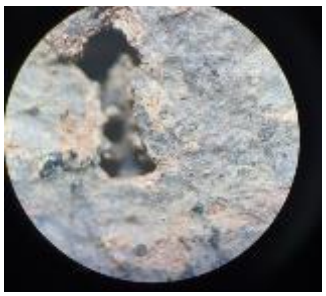
3		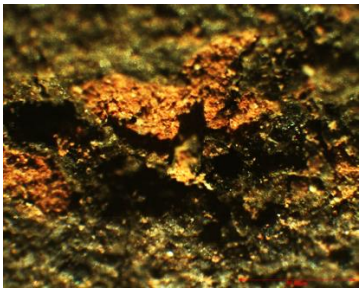	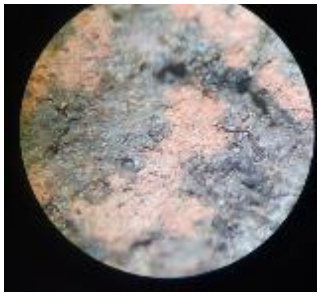

Table 1. *Cont.*

No. of Sample	Visual Aspect	Optical Microscopy	Stereomicroscopy
4			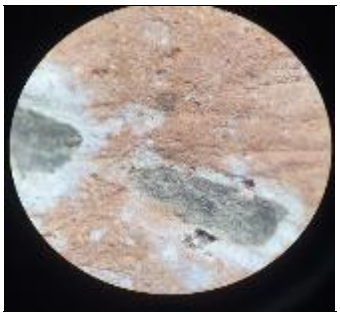
5			
6			
7A (white pigment)			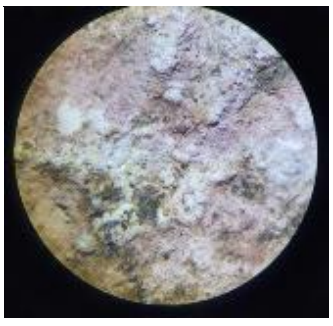

Table 1. *Cont.*

No. of Sample	Visual Aspect	Optical Microscopy	Stereomicroscopy
7B (red substrate)			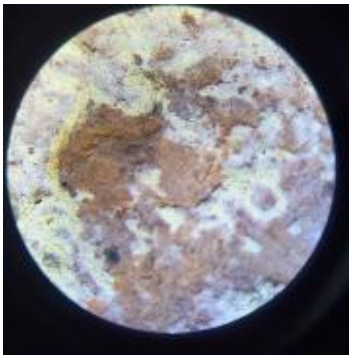

2.2. Equipments

For X-ray diffraction (XRD) measurements, a Rigaku Ultima IV X-ray diffractometer (Rigaku, Tokyo, Japan) was used with the following parameters: Cu-Kα radiation, wavelength λ = 0.15406 nm, 40 kV and 30 mA, scanning speed 2° min^{-1}, angular range 2θ = 5–80°. For efficient data processing, the Rietveld method was used for the correct identification of the components present in the samples.

The wavelength dispersive X-ray fluorescence spectroscopy (WDXRF) data were obtained with a Rigaku ZSX Primus II spectrometer (Rigaku, Tokyo, Japan) with a 4.0 kW Rh anode X-ray tube.

Fourier transform infrared spectroscopy (ATR-FTIR) was performed in the range of 4000–400 cm^{-1} with a Vertex 80 spectrometer (Bruker Optik GMBH, Billerica, MA, USA), where an attenuated total reflectance (ATR) accessory was used.

For the Raman spectroscopy measurements, a portable analyzer (Xantus-2, Rigaku, Woodlands, TX, USA) equipped with two types of 785 and 1064 nm laser was used, with a measurement range of 200–2000 cm^{-1}.

A Novex trinocular microscope (Euromex Microscopen B.V., Arnhem, The Netherlands) was used to view optical microscopy images (magnifications: 40, 100, 400, 1000×). The microscope was equipped with a digital video camera (Axiocam 105, Zeiss, Göttingen, Germany), in order to acquire data in real time.

For stereomicroscopy images, a trinocular microscope (EUROMEX Microscopen B.V., BD Arnhem, Netherlands), model 1903, with magnitudes of 7–45× was used.

For detailed images of the samples, the ambient scanning electron microscopy (ESEM) was used with the following operating modes: High vacuum (<1.3 Pa); low vacuum (10–130 Pa); ESEM (130–2600 Pae); SEM + EDS (energy dispersive spectroscopy).

A NOVA 2200e gas sorption analyzer (Quantachrome, Boynton Beach, FL, USA) was used to measure nitrogen adsorption/desorption isotherms, recorded at 77.35 K in the relative pressure range p/po = 0.005–1.0. Data processing was performed using NovaWin version 11.03 software. Before adsorption measurements, the samples were degassed at 120 °C under vacuum for 4 h.

For the specific area, a standard BET (Brunauer–Emmett–Teller) equation was used and the following criteria have been used: The total pore volume was estimated from the adsorbed volume at a w/po relative pressure close to unity. The pore size distribution and mesopore volume were obtained by applying the Barrett–Joyner–Halenda (BJH) model.

The thermogravimetric analysis of the investigated samples was recorded with a Pyris 1 TGA analyzer (Perkin Elmer TGA-7, Waltham, MA, USA), with the following working

parameters: Temperature regime 50–700 °C, heating rate of 10 °C/min, nitrogen bubbling, 50 mL/min flow rate.

For the chromatic parameters, a CR-410 colorimeter (Konica Minolta, Tokyo, Japan) was used, working in the CIE L*a*b* system (CIE 1986) [11].

3. Results and Discussion

The ceramics, as the most important archaeological artefact, always involve a series of important investigations for archaeologists, and the results obtained lead to useful conclusions, such as cultural groups, their location, and population movements in certain geographical areas [12]. These data result from the compositional evaluation of the ceramic paste and can support the archaeological discoveries investigated [13].

The samples selected for this study come from different groups of samples with different chemical compositions. Following the visual examination of the samples, it was possible to observe the variation in the color of the ceramic body from yellow-red to brown or red-brown-white or even black. In cross-section, the ceramic wall generally has a two-layer texture, with the outer layer having a lighter color and the inner layer being darker. The existence of this layer can be a good indicator of uneven firing over the entire body of the pottery (insufficient firing time for the organic material in the clay to have burned), and may be an indication of firing the pottery in a reducing atmosphere followed by a final stage of rapid oxidation [14,15].

3.1. WDXRF and XRD

The WDXRF measurements allow for an approximate identification of the investigated samples (Table 2). Intensity distribution maps show the presence of calcium and small amounts of elements Al, Na, K, Si, Ti, and Fe, which may indicate the presence of minerals rich in these elements, such as silicates, calcite, K-feldspar, hematite, etc. [16].

The samples were investigated by X-ray diffraction to identify the main mineral phases, as well (Figure 2).

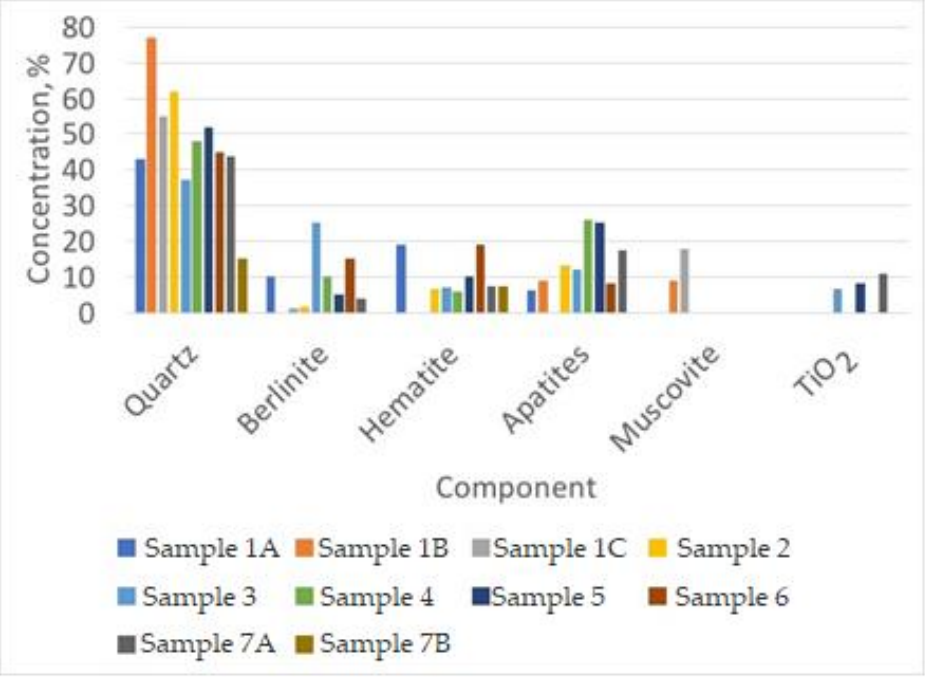

Figure 2. XRD registrations for the investigated pottery.

Table 2. Mineral composition (WDXRF) of the pottery fragments, expressed in mass% ± SD%, normalized to 100% *.

Sample	Sample 1	Sample 2	Sample 3	Sample 4	Sample 5	Sample 6	Sample 7A	Sample 7B
Component	Result, %	Result, %	Result, %	Result, %	Result, %	Result, %	Result, %	Result, %
Na_2O	0.876 ± 0.33271	1.1547 ± 0.44055	1.3335 ± 0.42345			1.7769 ± 0.5086	0.9163 ± 0.352	5.7411 ± 0.35973
MgO	2.1174 ± 0.13284	2.6104 ± 0.19126	2.5734 ± 0.18539	3.526 ± 0.22631	2.7062 ± 0.18788	3.4099 ± 0.23444	3.265 ± 0.16829	2.447 ± 0.15046
Al_2O_3	20.5967 ± 0.08506	20.4475 ± 0.10211	22.1634 ± 0.11004	22.5278 ± 0.11852	23.9212 ± 0.1065	24.3272 ± 0.12217	23.8336 ± 0.1064	22.041 ± 0.08856
SiO_2	63.0808 ± 0.13654	60.6971 ± 0.15081	59.9206 ± 0.14352	53.9348 ± 0.15167	56.1471 ± 0.15129	50.9206 ± 0.16784	48.6089 ± 0.12867	54.4279 ± 0.12469
P_2O_5	0.5403 ± 0.02831	2.799 ± 0.03708	1.4651 ± 0.03321	3.366 ± 0.04292	3.8759 ± 0.0394	3.7408 ± 0.04458	8.3896 ± 0.04326	1.2258 ± 0.02505
SO_3	0.043 ± 0.0155		0.078 ± 0.01842		0.061 ± 0.0198	0.0679 ± 0.02521	0.045 ± 0.02249	0.0447 ± 0.0145
Cl		0.0176 ± 0.00765	0.0252 ± 0.00809	3.0729 ± 0.03897		0.0134 ± 0.01164		0.0866 ± 0.00615
K_2O	2.5105 ± 0.02635	2.5185 ± 0.03583	2.6434 ± 0.03266	2.9618 ± 0.0386	2.9934 ± 0.03895	2.8486 ± 0.04633	2.1593 ± 0.03178	2.7978 ± 0.02536
CaO	1.2381 ± 0.02204	1.6337 ± 0.02754	1.5515 ± 0.02681	3.0729 ± 0.03897	1.579 ± 0.02999	1.8524 ± 0.03778	3.8639 ± 0.03292	5.093 ± 0.02779
TiO_2	0.8534 ± 0.04482	0.9166 ± 0.06044	0.7303 ± 0.04474	1.0762 ± 0.05902	0.8335 ± 0.06292	1.0161 ± 0.07512	0.7801 ± 0.03887	0.6776 ± 0.05389
Cr_2O_3	0.0413 ± 0.0211			0.0637 ± 0.0241			0.0588 ± 0.02647	
MnO	0.1393 ± 0.01759	0.1779 ± 0.01835	0.196 ± 0.0166	0.1235 ± 0.02397	0.1202 ± 0.01731	0.1757 ± 0.02248	0.1669 ± 0.02335	0.1135 ± 0.01396
Fe_2O_3	7.8166 ± 0.01663	6.986 ± 0.02827	7.2758 ± 0.01993	9.2826 ± 0.0272	7.7043 ± 0.02522	9.7643 ± 0.02909	7.8634 ± 0.02673	5.2828 ± 0.02306
ZnO	0.0146 ± 0.00807	0.0253 ± 0.00981	0.0278 ± 0.01166	0.0295 ± 0.01434	0.029 ± 0.01098	0.0533 ± 0.01633	0.0333 ± 0.01168	
Rb_2O	0.0212 ± 0.00547	0.0157 ± 0.00744	0.0159 ± 0.00698	0.0352 ± 0.00844	0.0294 ± 0.00958	0.033 ± 0.01227	0.0159 ± 0.00847	

* WDXRF data obtained by EZ scan analysis, in vacuum, in powder, the pellets (1.5 g of sample mixed with 2 g BOREOX—FLUXANA).

It is important to note that the investigated samples are completely heterogeneous, and the nomenclature of the identified minerals complies with the IMA-CNMNC approved list [16]. Quartz and berlinite were identified, followed by hematite, anorthite, sodalite, scorzalite, albite, apatite, muscovite, mica, feldspar, crotite, TiO_2, and graphite (Figure 2). Despite those identified in our work (only aluminum phosphate (berlinite)), in other publications, only hydroxyapatite (calcium phosphate) was reported as a source of phosphate [17]. In the investigated samples from this paper, calcium is not present as a major component as raw material. Only in a few samples calcium could be identified, as calcite, phosphate or sulfate forms, and in very small concentrations, most probably from the clay existing here. This could be correlated with the different geological formations present in the areas where the investigated archaeological sites are located. During the investigations carried out, the ceramic shards from the archaeological site were analyzed by WDXRF and the Fe-Ca concentrations for the clay body from all the studied samples. Almost all samples show a low Ca concentration indicating the use of raw materials with a low limestone content (poor Ca clays) for the manufacture of these ceramics. In general, clays with a CaO concentration of less than 5% (Ca < 3.6%) are considered as non-calcareous [14]. Regarding the Fe concentration in the clay paste of the samples, it is between 5% and 8% in almost all samples. Low concentrations of hematite have been identified.

The presence of calcite can be used for provenance studies of ceramics, since alteration processes can affect the presence of elements, such as alkaline elements Na, K, Rb, and Cs [18,19]. Calcite can be a good indicator of the firing temperature of a ceramic material, and the identification of calcite serves to identify the decomposition temperature. Moreover, it is very important to evaluate whether the calcite is in the presence or absence of some silicates. In the presence of some silicates, during the prolonged firing of ceramics, the decarbonation process takes place at temperatures between 600 and 800 °C, to form possible silicates (for example, gehlenite), above or around 800 °C [20]. The presence of calcite without newly formed silicates indicates firing around 800 °C, while the presence of newly formed silicates, such as gahlenite indicates firing well above 800 °C. The presence of calcium in these low concentrations (below 5%) is a criterion for defining the upper limit of the firing temperature, concluding that the pottery was fired below the decarbonation temperature of this mineral. These observations are valid only when calcite is present in the ceramic. For example, its ability to react or not with the other elements and form gahlenite indicates the decomposition of calcite and its implications for the respective ceramics. In the case investigated by us, no gahlenite-type compounds were identified by XRD; therefore, the calcite present here is silicate-free, and the upper limit of calcite decomposition is in the range of 600–800 °C [21].

The white material present below the red variscite layer was identified by the 2-theta peaks in XRD attributed to quartz, with some berlinite components and a minor amount of calcite. According to Rietvelt processing, the identified phases were: Berlinite, with 2θ peaks at 21.02° and 26.79°; quartz with peaks at 20.85°, 26.65°, and 28.2°; calcite/dolomite with peaks at 30° and 38°, as well as small amounts of the feldspar group (alkali and alkaline earth metal cations containing aluminosilicate) (Figure 3).

The results show that Ca-rich minerals (calcite) were used for the white color, while different types of Fe-rich minerals (ochre) were identified by the red colors. Dark brown colors were mostly prepared using Mn-rich minerals; however, in one case, we found the dark brown color prepared with Fe-rich minerals, which was probably released in the reducing atmosphere. The black part of the samples should probably have been prepared after burning with bitumen, since the black area is rich in sulfur with traces of vanadium (<0.005%). It should be noted that similar types of pigments have been found by other researchers on Neolithic pottery from various sites in the Balkans and Europe [18].

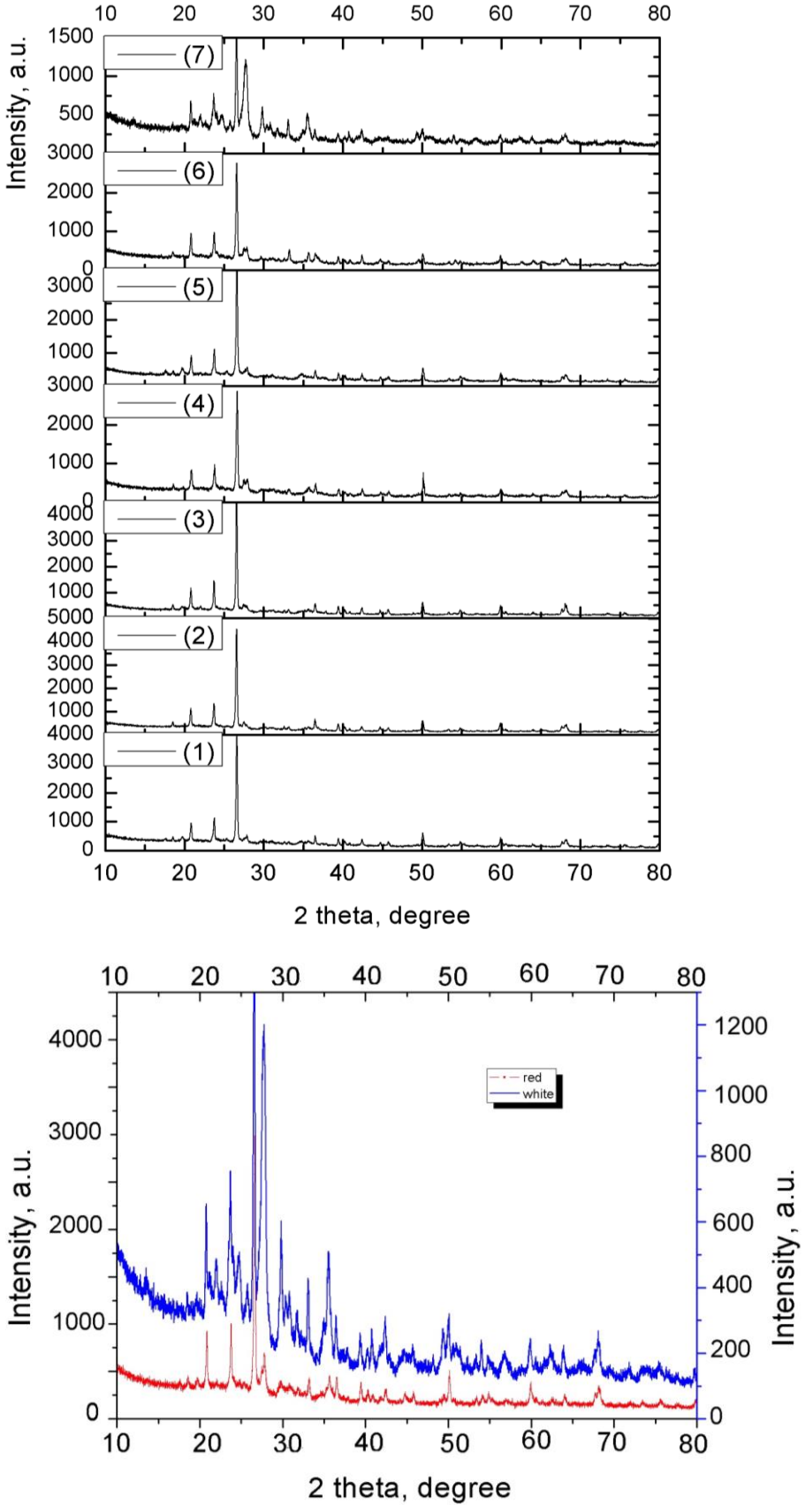

Figure 3. XRD spectra for the ceramic substrate (red) and the white encrustation. The explanation of (1)–(7) is the same with the codification from Table 1.

Another explanation for the poor constitution of the ceramics found here lies in the possible application of hydraulic lime, whose property of hardening in water is maximized when it includes a clay content of 20%–22% (about 5% magnesium oxide), which can be obtained naturally by calcining calcareous marls [19].

Berlinite, $AlPO_4$, is a rare high-temperature aluminum phosphate mineral with a quartz-like crystal structure. Berlinite is present only in a few localities worldwide, and in association with metamorphic or hydrothermally altered rocks [20–23]. The system Al_2O_3-$AlPO_4$-H_2O was reported for the first time in Romania by Onac [24].

Berlinite could be generated from variscite ($AlPO_4 \cdot 2H_2O$) or from gypsite ($Al(OH)_3$) via bat guano by the microbiological method; the hydrothermal method can be excluded in this case since the 550 °C temperature when berlinite is generated is difficult to be explained in soil. The acidic solutions rich in phosphates released from the guano must also be considered, which react with the aluminum-rich clays present as underlying fluvial sediments or cave dust through microbial action, in order to produce hydrated aluminum phosphate. According to some sources, berlinite is almost certainly the product of microbial biochemical reactions on the surface of variscite crystals, transforming into berlinite through water loss. A bacterial colonization of the surfaces of many plasters has been identified according to the literature [25].

Microscopic examinations in thin section show that, in general, a ceramic made of semi-final clays with amorphous-microcrystalline structure with several voids of spherical and elliptical shape, as well as various natural non-plastic inclusions, belong to the raw materials or were added as temperament. Various inclusions are generally angular to the subangular and range in size from 1 to 3 mm. They constitute 5%–10% of the sample volume. Non-plastic inclusions are mainly composed of quartz, plagioclase, mica (muscovite), calcite, and opaque minerals represented by hematite. All these formations could be observed in SEM images (Figure 4).

SEM micrograph was used to study the microstructure of the samples with different compositions (Figure 4). In the case investigated in this paper, the SEM analysis showed that the material is composed of a loose powder (Figure 4A,B), with tiny particles of approximately 100 nm (at the limit of SEM resolution). Spherulitic variscite is present as gibbsite or berlinite (Figure 4C–F). Energy dispersive spectroscopy (EDS) served as the chemical characterization of the geopolymerization products. The surface of the sample is covered with individual "rose-shaped" crystals typical of hydrosodalite with a size of about 1.5 μm [26–28]. Samples based on red brick waste had the highest coverage of hydrosodalite crystals.

The EDS test results are shown in Figure 5. The oxygen content of the AAM matrix was from 59 to 61 wt%, aluminum from 6.2 to 7.6 wt%, silicon from 16.7 to 19.9% by weight, and Na from 7.9 to 10.5% by weight.

The EDS results indicate that there is a relatively similar content for all blends. Compared to metakaolin-based geopolymers that have O from 41% to 43%, aluminum from 11.6 to 16.5 wt%, silicon from 24.5 to 26 wt%, and sodium from 5.2 to 7.4 wt%, oxygen and sodium content increased, while aluminum and silicon content decreased [29].

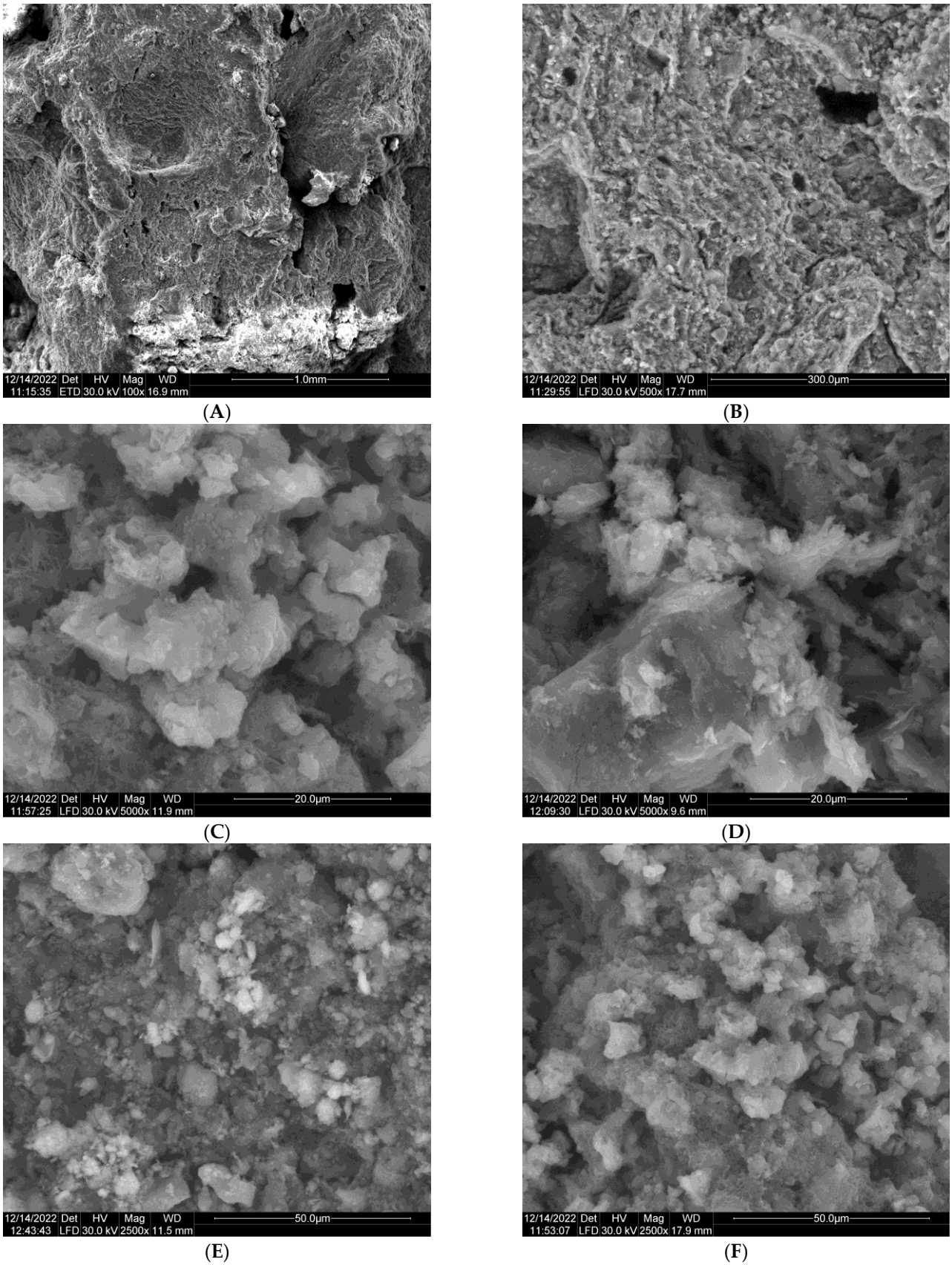

Figure 4. SEM images of the pottery, red area (**A**,**B**) and white area (**C**–**F**).

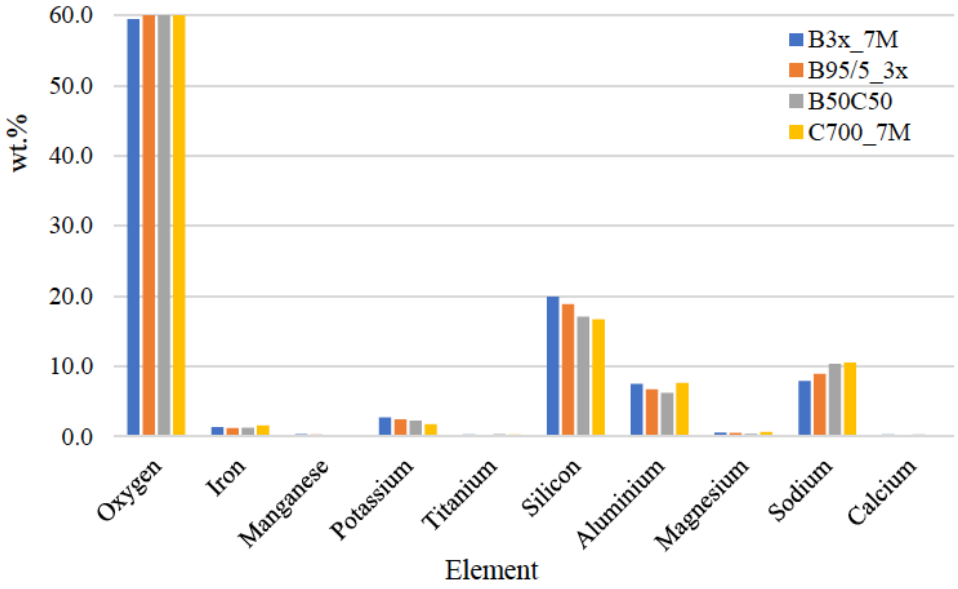

Figure 5. EDS analysis for the investigated samples.

3.2. Chromatic Parameters

From the material analysis, it could be observed that the obtained ceramics have different colors, depending on the burning processes. Some of these processes are visible by darker colors, as determined by chromatic parameters (Figure 6).

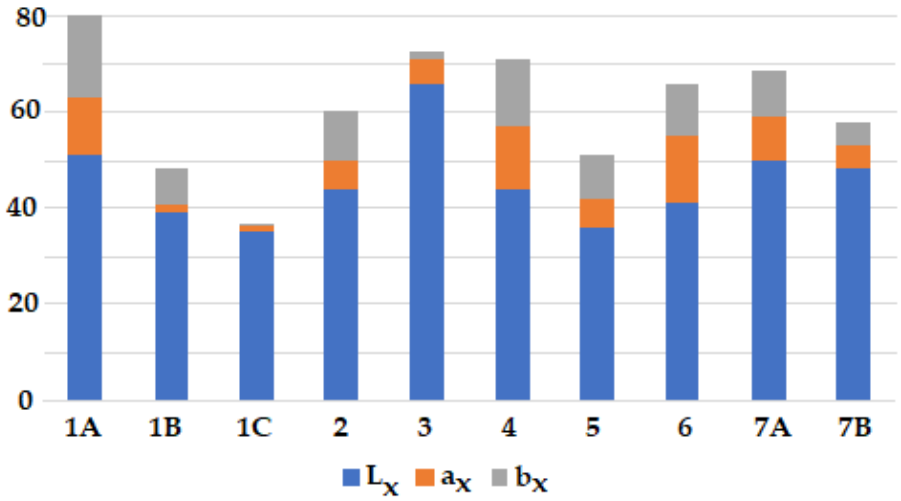

Figure 6. The chromatic parameters of the pottery samples.

By analyzing Figure 6, it could be concluded that the smaller the a_x and b_x range, the closer the red colors are observed. L_x is approximatively the same for all samples.

3.3. Thermogravimetry

The thermal stability of the samples, recorded up to 700 °C, is shown in Figure 7.

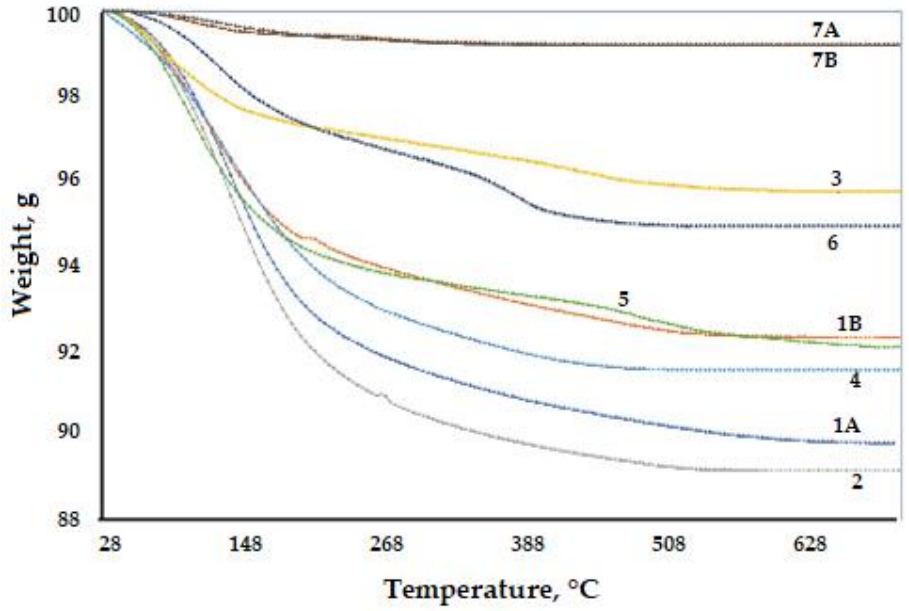

Figure 7. Thermogravimetric analysis of the investigated samples.

Between 100 and 250 °C, the absorption water specific to each clay deposit is removed, followed by the removal of chemically bound water up to a temperature of 400 °C. Exceeding these intervals creates the possibility of a rapid rise in temperature to close to the maximum values specific to each type of clay, when vitrification of the clay mass and deformation of the parts occur. The characteristic temperature conditions for the vessel color are the light brown color which appears at 600 °C, while the pink color appears at 800–900 °C.

After burning, only one piece suffered physical accidents due to the sudden evaporation of water, resulting in circular exfoliation in some areas of the walls. A small mass weight decrease was observed from the thermogravimetric analysis, with the clay transformed into ceramics.

Usually, the presence of calcite is an indicator of the low burning temperature, but in our case, calcium is found only in a few samples and in low concentrations, as we have shown above.

On the other hand, iron oxides play the most important role in the burning atmosphere, the burning of iron-rich clay in reducing conditions (absence of oxygen in the furnace) leads to blackened samples, and those in which burning takes place in oxidizing conditions lead to reddish samples.

The presence of calcite in pottery may occur due to the low firing temperature. Calcite exists up to ~800 °C, when CaO appears, followed by the formation of a complex phase consisting of Ca-silicates or Ca,Al-silicates, including plagioclases (for example, anorthite $CaAl_2Si_2O_8$) [30], or even gahlenite, as we previously mentioned.

According to the obtained results, the investigated samples contain non-calcareous clay as calcium in found in low concentrations.

3.4. Porosity

Porosity for different textured samples could be an important attribute of ancient pottery and could offer information about the firing temperature, the type of clay and tempering materials, and the manufacturing and forming techniques employed [31].

Textural measurements were performed to investigate changes in this property as a function of composition. The specific surface varies between 39.4 and 58.6 m^2/g. The white sample 7A has a higher specific surface, which suggests that the firing temperature of the material was lower, knowing that those amounts of calcite in the ceramic compo-

sition reduce shrinkage during firing [32]. The mesopore size distribution using the BJH method [33], which uses the modified Kelvin equation (Figures 8 and 9), indicates that the pore diameter in each sample varies between 2 and 5 nm, with a maximum distribution toward 4 nm. The ceramic body has all the porosity parameters at half the value compared to the white inlay, this being proof of its stability, due to the metallic phosphate present in the composition (Table 3).

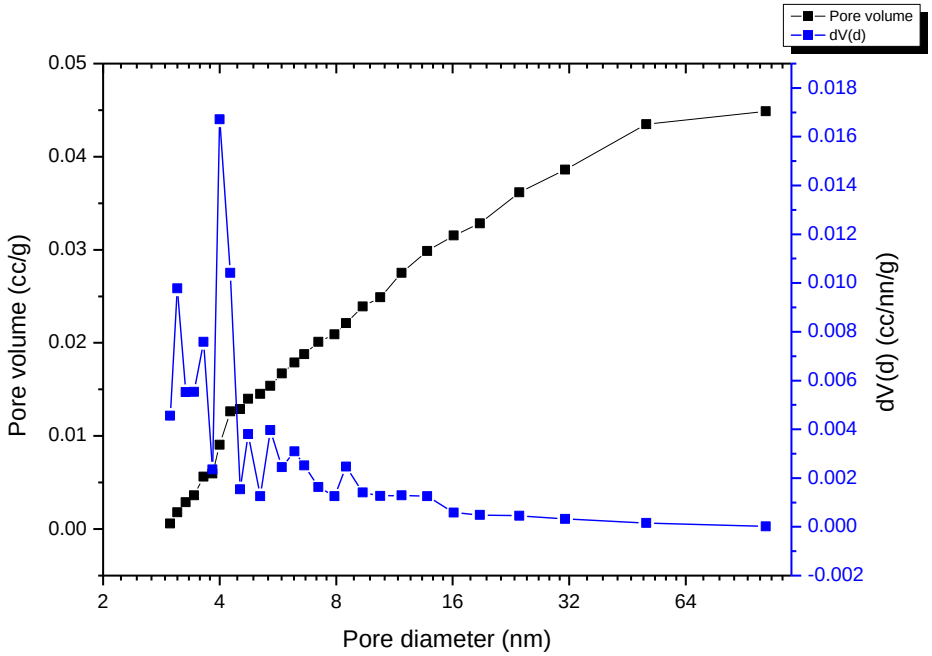

Figure 8. BJH desorption of the 7A (white sample).

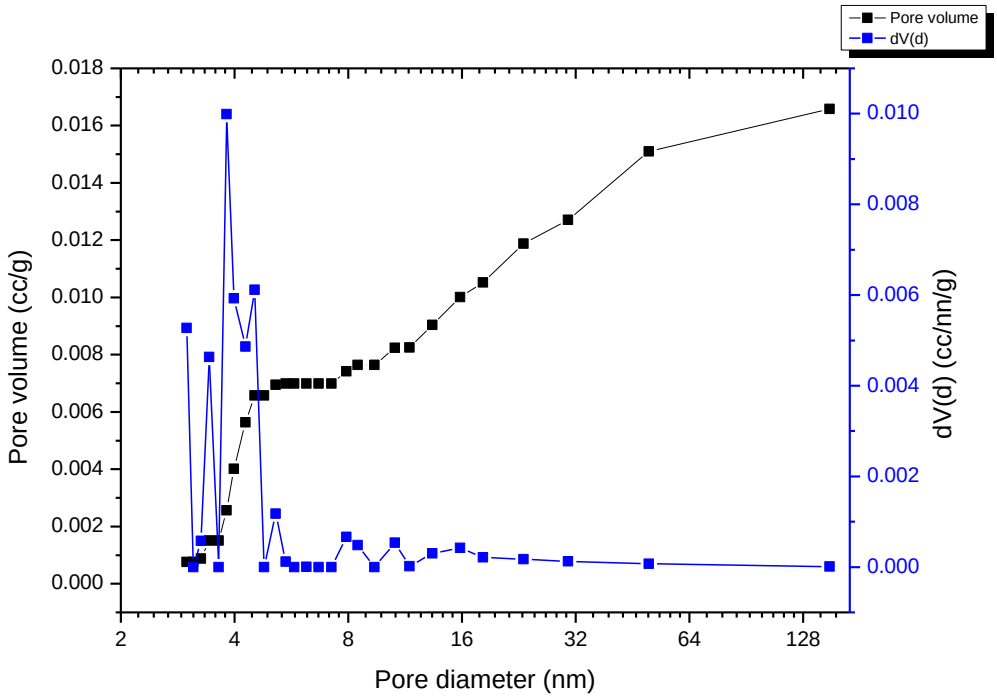

Figure 9. BJH desorption of the 7B (red sample).

Table 3. The porosity parameters for the investigated samples.

No.	Sample	Specific Area (m^2/g)	Total Pore Volume (cm^3/g)	Average Pore Diameter (nm)
1	7A (white)	58.54	0.0605	4.133
2	7B (red)	39.38	0.0288	2.99

3.5. FTIR

The mineralogy of the samples can be shown by FTIR and Raman. The spectra highlighted the bands assigned to carbonate phases (1800 cm^{-1}, 1406–1440 cm^{-1}, 873 cm^{-1}, and 711 cm^{-1}) and bound water (bands at 3370 and 1630–1640 cm^{-1}), which are most probably related to hydraulic compounds, such as silicates and aluminate hydrates (strong silicate (Si–O) bands at 1011–1022 cm^{-1}) and Al–O bands around 1000 cm^{-1} characterizing internal Si–O-Si (asymmetric stretching) and Si-O-Al bonds [34].

FTIR spectra recorded on the same samples show berlinite, calcite, and quartz peaks. The absorption peaks of calcite are related to the strong peak (CO_3) at ~1391 cm^{-1} (asymmetric stretching mode ν3), accompanied by two sharper peaks at ~713 cm^{-1} (strain mode ν1) and ~874 cm^{-1} (symmetric ν2 mode). Smaller peaks (CO3) related to berlinite are observed at higher energies above 1500 cm^{-1} (Figure 10). There are two strong peaks characteristic of phosphate groups at 1048 and 1087 cm^{-1} attributed to asymmetric ν3 stretching modes of (PO_4) and a significantly weaker peak at 962 cm^{-1} associated with symmetric ν1 stretching of (PO_4) groups. The peaks at 562 and 598 cm^{-1} are due to the asymmetric ν4 bending mode of (PO4), a smaller peak at 631 cm^{-1} due to hydroxyl groups, a few weaker peaks due to carbonate groups, as follows: Peak at 875 cm^{-1}, which is assigned to the symmetric ν2 mode of the (CO_3) groups and the 1414 and 1458 cm^{-1} bands assigned to the asymmetric ν3 stretching modes of (CO_3).

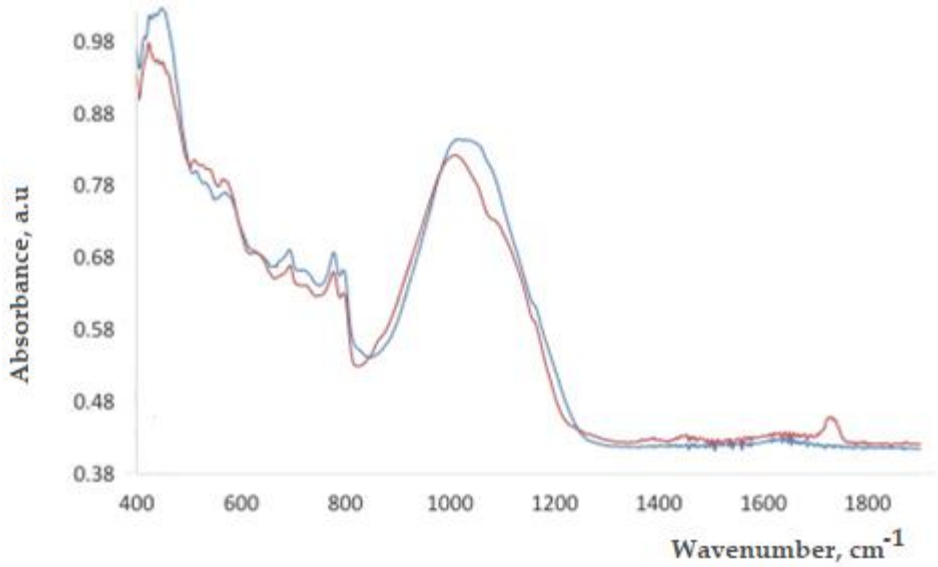

Figure 10. FTIR spectra of the red substrate and white deposits (encrustation) (red line—white powder; blue line—red ceramic).

The presence of quartz can be evidenced by the bending vibration at 694 cm^{-1}, the doublet at 777 and 796 cm^{-1} (stretching vibration bands), characteristic absorptions for Si-O, and the bands at 413–460 cm^{-1}. Crystalline quartz is highlighted by the broad band around 1000 cm^{-1} [35].

3.6. Raman

The Raman spectroscopy is an important technique in the field of cultural heritage, history, and art. Materials for ceramics, such as quartz, feldspars, carbonate, and iron oxides are well-characterized by their Raman spectra, and thus a detailed mineralogical composition can be obtained easily [36–43]. The results obtained during our tests, led to the following attributions, Figures 11 and 12:

- Frequency of the phosphate group in the region 1230–1060 and 530–360 cm^{-1};
- aluminum is located in the region of 740–570 cm^{-1};
- quartz is characterized by a prominent peak at 467 cm^{-1} and a peak of medium intensity at 210 cm^{-1};
- K-feldspars and plagioclases may still be possible; the first group shows characteristic lines almost centered at 455, 475, and 513 cm^{-1};
- rutile can be identified at 440 and 610 cm^{-1}.

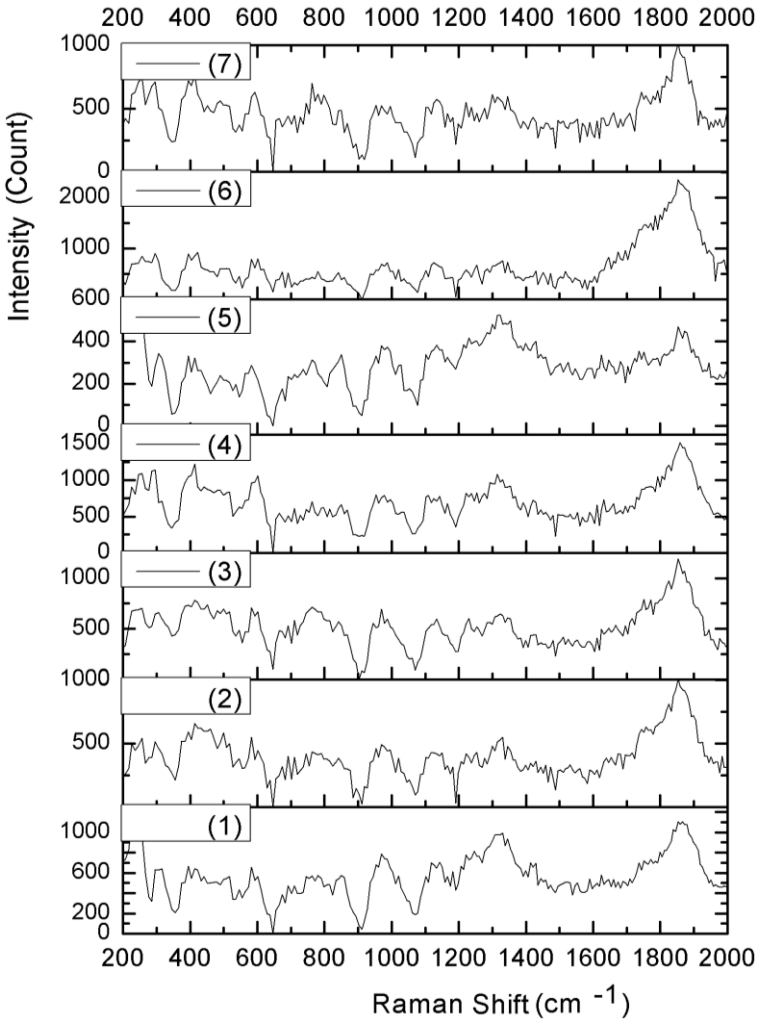

Figure 11. Raman spectra for the investigated samples. The explanation of (1)–(7) is the same with the codification from Table 1.

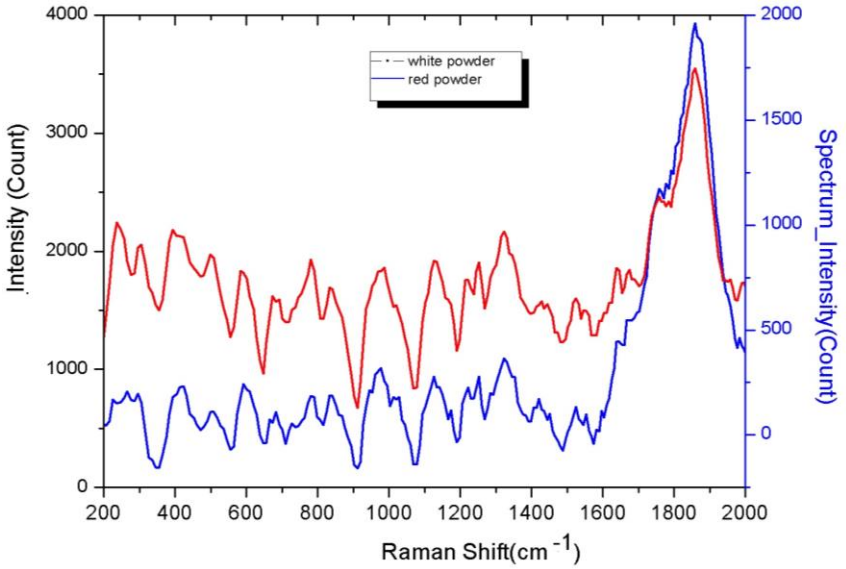

Figure 12. Raman spectra of white powder (blue line) and red ceramic (red line).

4. Conclusions

In this paper, the pottery fragments composition and white pigments encrusted on the incised pottery are herein included. Some archaeometric investigations were carried out by the WDXRF method for chemical composition, XRD and FTIR for mineralogical data, OM/stereomicroscopy/SEM for microstructure and morphology observation. XRD examinations have shown that the ceramics are generally made of quartz, berlinite, muscovite, calcite, and opaque minerals, such as hematite. All evidence indicates the use of raw materials with a low limestone content (poor Ca clays) for the manufacture of these ceramics (Ca < 3.6%). X-ray fluorescence (XRF) measurements indicated various concentrations of Al, Si, Fe, Ca, and Zn and decreased concentrations of P, Sr, and K. From the BJH desorption diagrams of the samples, a series of pores with dimensions between 2 and 5 nm are noted.

The white pigment encrusted with white color contains calcite, gypsum, clays, and quartz, as well as carbon deposits in the pores of the pottery, all specific to the Chalcolithic ceramics from this region. The FTIR spectra recorded on the same samples led to the identification of phosphatic minerals, calcite, and quartz, through the specific absorption peaks of calcite, quartz, gypsum, and aluminum phosphate, present as berlinite in all the pottery specific to this area.

Author Contributions: Conceptualization, R.-M.I.; methodology, R.-M.I., V.D. and G.V.; software, G.V.; validation, R.-M.I., V.D. and G.V.; formal analysis, V.D.; investigation, R.-M.I., V.D., G.V., L.I., R.M.G., A.I.G., L.-A.M., E.A. and S.S.-T.; resources, R.-M.I.; writing—original draft preparation, R.-M.I.; writing—review and editing, R.-M.I.; visualization, V.D. and G.V.; supervision, R.-M.I., V.D. and G.V.; project administration, R.-M.I.; funding acquisition, R.-M.I. All authors have read and agreed to the published version of the manuscript.

Funding: This paper received the financial support of the project: PN-III-P2-2.1-PED-2021-3885 from UEFISCDI-MCID, Romania.

Institutional Review Board Statement: Not applicable.

Informed Consent Statement: Not applicable.

Data Availability Statement: The data presented in this study are available on request from the corresponding author.

Conflicts of Interest: The authors declare no conflict of interest.

References

1. Mățău, F.; Chișcan, O.; Pintilei, M.; Garvăn, D.; Stancu, A. Technological features of the chalcolithic pottery from Târpești (Neamț County, Eastern Romania). *Mediterr. Archaeol. Archaeom.* **2019**, *19*, 93–104.
2. Diaconu, V. Recunoașteri arheologice de suprafață în zona orașului Târgu Neamț. *Mem. Antiq.* **2007**, *24*, 87–119.
3. Preoteasa, C.; Diaconu, V.; Mischka, D.; Mischka, C.; Praschl, B.; Schaffer, M.; Wanka, F.; Gapp, F. *Topolița, com. Grumăzești, jud. Neamț. Punct: La Nord-Vest de Sat, in Cronica Cercetărilor Arheologice din România. Campania 2016*; Institutul Național al Patrimoniului: Bucharest, Romania, 2017; p. 237.
4. Diaconu, V.; Gafincu, A.-M.; Hanceanu, G.D.; Nicola, C.-D.; Preoteasa, C.; Stiglet, D.-I.; Pirnau, R. *Topolița, com. Grumăzești, jud. Neamț. Punct: La Nord-Vest de sat, in Cronica Cercetărilor Arheologice din România. Campania 2018*; Institutul Național al Patrimoniului: Bucharest, Romania, 2019; pp. 392–397.
5. Pîrnău, R.G.; Patriche, C.V.; Roșca, B.; Mirea, D.A.; Diaconu, V.; Stan, C.O.; Bobric, E.D.; Vasiliniuc, I.; Mănăilescu, C.; Rusu, C. Insights into the Phaeozems pedogenesis using total elemental composition analysis. A case study from north-eastern Romania. *Geoderma* **2022**, *409*, 115604. [CrossRef]
6. Ion, R.-M.; Barbu, M.G.; Gonciar, A.; Vasilievici, G.; Gheboianu, A.I.; Slamnoiu-Teodorescu, S.; David, M.E.; Iancu, L.; Grigorescu, R.M. A Multi-Analytical Investigation of Roman Frescoes from Rapoltu Mare (Romania). *Coatings* **2022**, *12*, 530. [CrossRef]
7. Ion, R.-M.; Ion, M.-L.; Fierascu, R.; Serban, S.; Dumitriu, I.; Radovici, C.; Bauman, I.; Cosulet, S.; Niculescu, V. Thermal analysis of Romanian ancient ceramics. *J. Therm. Anal. Calorim.* **2010**, *102*, 393–398. [CrossRef]
8. Ion, R.M.; Iancu, L.; David, M.E.; Grigorescu, R.M.; Trica, B.; Somoghi, R.; Vasile, S.F.; Dulama, I.D.; Gheboianu, A.I.; Tincu, S. Multi-Analytical Characterization of Corvins' Castle—Deserted Tower. Construction Materials and Conservation Tests. *Heritage* **2020**, *3*, 941–964. [CrossRef]
9. Ion, R.-M.; Tincu, S.; Minca, I.; Dulama, I.; Bucurica, I.; Ion, M.; Gheboianu, A. Instrumental Analytical Techniques Applied to Old Gate Tower from Corvins' Castle. *IOP Conf. Ser. Mater. Sci. Eng.* **2020**, *877*, 012050. [CrossRef]
10. Ion, R.-M.; Fierăscu, R.-C.; Teodorescu, S.; Fierăscu, I.; Bunghez, I.-R.; Ţurcanu-Caruţiu, D.; Ion, M.-L. Ceramic materials based on clay minerals in cultural heritage study. *Clays Clay Miner. Ceram. Mater. Based Clay Miner.* **2016**, *26*, 159–184.
11. *ISO/CIE 11664-2:2022*; Colorimetry—Part 2: CIE Standard Illuminants. ISO: Geneva, Switzerland, 2006.
12. Ion, R.-M.; Ion, M.L.; Fierascu, R.C.; Dumitriu, I.; Rugina, F.; Niculescu, V.I.R. Studii de arheometrie asupra unor artefacte ceramice din patrimoniul muzeal românesc. *Bul. Univ. Valahia Din Targoviste–Sect. Ing. Mater. Si Mecatronica* **2007**, *5*, 62–68.
13. Bishop, R.L.; Rands, R.L.; Holley, G.R. Ceramic compositional analysis in archaeological perspective. In *Advances in Archaeological Method and Theory*; Elsevier: Amsterdam, The Netherlands, 1982; pp. 275–330.
14. Tite, M.S. Ceramic production, provenance and use—A review. *Archaeometry* **2008**, *50*, 216–231. [CrossRef]
15. Rice, P.M. *Pottery Analysis: A Sourcebook*; University of Chicago press: Chicago, IL, USA, 2015.
16. Ion, R.-M.; Iancu, L.; Grigorescu, R.M.; Slamnoiu-Teodorescu, S.; Dulama, I.D.; Bucurica, I.A. Degradation Products Assessment of the Wooden Painted Surfaces from a XVIIth Heritage Monastery. *Appl. Sci.* **2023**, *13*, 2124. [CrossRef]
17. Warr, L. IMA-CNMNC approved mineral symbols. *Mineral. Mag.* **2021**, *85*, 1–35. [CrossRef]
18. Buxeda, I.; Garrigos, J.; Kilikoglou, V.; Day, P.M. Chemical and mineralogical alteration of ceramics from a Late Bronze Age kiln at Kommos, Crete: The effect on the formation of a reference group. *Archaeometry* **2001**, *43*, 349–371.
19. Schwedt, A.; Mommsen, H.; Zacharias, N.; Buxeda i Garrigos, J. Analcime crystallization and compositional profiles—Comparing approaches to detect post-depositional alterations in archaeological pottery. *Archaeometry* **2006**, *48*, 237–251. [CrossRef]
20. Iordanidis, A.; Garcia-Guineab, J.; Karamitrou-Mentessidic, G. Analytical study of ancient pottery from the archaeological site of Aiani, northern Greece. *Mater. Charact.* **2009**, *60*, 292–302. [CrossRef]
21. Maggetti, M.; Neururer, C.; Ramseyer, D. Temperature evolution inside a pot during experimental surface (bonfire) firing. *Appl. Clay Sci.* **2011**, *53*, 500–508. [CrossRef]
22. Fabbri, B.; Gualtieri, S.; Shoval, S. The presence of calcite in archeological ceramics. *J. Eur. Ceram. Soc.* **2014**, *34*, 1899–1911. [CrossRef]
23. Opriș, V.; Velea, A.; Secu, M.; Rostas, A.-M.; Buruiană, A.-T.; Simion, C.-A.; Mirea, D.-A.; Matei, E.; Bartha, C.; Dimache, M. 'Put variety in White': Multi-analytical investigation of the white pigments inlaid on Early Chalcolithic pottery from Southern Romania. *J. Archaeol. Sci. Rep.* **2022**, *42*, 103402. [CrossRef]
24. Ndreçka, E.; Civici, N.; Beqiraj, E.; Gjipali, I. Results from Multi Technique Investigation of Pottery from Different Early Neolithic Sites in Albania. *J. Mater. Sci. Chem. Eng.* **2017**, *5*, 10–26. [CrossRef]
25. Agresti, J.; Indelicato, C.; Perotti, M.; Moreschi, R.; Osticioli, I.; Cacciari, I.; Mencaglia, A.A.; Siano, S. Quantitative Compositional Analyses of Calcareous Rocks for Lime Industry Using LIBS. *Molecules* **2022**, *27*, 1813. [CrossRef]
26. Duggan, M.B.; Jones, M.T.; Richards, D.N.; Kamprad, J.L. Phosphate minerals in altered andesite from Mount Perry, Queensland, Australia. *Can. Mineral.* **1990**, *28*, 125–131.
27. Ek, R.; Nysten, P. Phosphate mineralogy of the Hålsjöberg and Hökensås kyanite deposits. *Geol. Foereningen Stockh. Foerhandlingar* **1990**, *112*, 9–18. [CrossRef]
28. Gallagher, M.; Gerards, J. Berlinite from Rwanda. *Mineral. Mag. J. Mineral. Soc.* **1963**, *33*, 613–615. [CrossRef]
29. Reif, J. Berlinite, AlPO_4, from sulphide ore deposit Zlate Hory West. *Chasopis Miner. Geol.* **1989**, *34*, 363–372.
30. Onac, B.P.; White, W.B. First reported sedimentary occurrence of berlinite (AlPO4) in phosphate-bearing sediments from Cioclovina Cave, Romania. *Am. Mineral.* **2003**, *88*, 1395–1397. [CrossRef]

31. McFarlane, D.A.; Lundberg, J. New records of guano-associated minerals from caves in northwestern Borneo. *Int. J. Speleol.* **2018**, *47*, 119–126. [CrossRef]
32. Zong, Y.-B.; Zhao, C.-Y.; Chen, W.-H.; Liu, Z.-B.; Cang, D.-Q. Preparation of hydro-sodalite from fly ash using a hydrothermal method with a submolten salt system and study of the phase transition process. *Int. J. Miner. Metall. Mater.* **2020**, *27*, 55–62. [CrossRef]
33. Albidah, A.; Alghannam, M.; Abbas, H.; Almusallam, T.; Al-Salloum, Y. Characteristics of metakaolin-based geopolymer concrete for different mix design parameters. *J. Mater. Res. Technol.* **2021**, *10*, 84–98. [CrossRef]
34. Fernández-Jiménez, A.; Cristelo, N.; Miranda, T.; Palomo, Á. Sustainable alkali activated materials: Precursor and activator derived from industrial wastes. *J. Clean. Prod.* **2017**, *162*, 1200–1209. [CrossRef]
35. Kozhukhova, N.; Zhernovskaya, I.; Teslya, A.Y.; Kozhukhova, M.; Yakovlev, E. High temperature effect on structure formation and performance of hybrid geopolymers. *J. Phys. Conf. Ser.* **2019**, *1353*, 012066. [CrossRef]
36. Maggetti, M. Phase analysis and its significance for technology and origin. In *Archaeological Ceramics*; Olin, J.S., Franklin, A., Eds.; Smithsonian Institution Press: Washington, DC, USA, 1982; pp. 121–133.
37. Dolenec, S.; Lux, J. Spectroscopic and porosimetric analyses of Roman pottery from an archaeological site near Mošnje, Slovenia. *Mater. Tehnol.* **2015**, *49*, 503–508. [CrossRef]
38. Lira, C.; Fredel, M.C.; da Silveira, M.D.; Alarcon, O.E. Effect of carbonates on firing shrinkage and on moisture expansion of porous ceramic tiles. In Proceedings of the Qualicer 98: V World Congress on Ceramic Tile Quality, Castellon, Spain, 8–11 March 1998; pp. 101–106.
39. Barrett, E.P.; Joyner, L.G.; Halenda, P.P. The determination of pore volume and area distributions in porous substances. I. Computations from nitrogen isotherms. *J. Am. Chem. Soc.* **1951**, *73*, 373–380. [CrossRef]
40. Kumar Mishra, A.; Mishra, A.; Anshumali. Geochemical characterization of bricks used in historical monuments of 14–18th century CE of Haryana region of the Indian subcontinent: Reference to raw materials and production technique. *Constr. Build. Mater.* **2021**, *269*, 121802. [CrossRef]
41. Hlavay, J.; Jonas, K.; Elek, S.; Inczedy, J. Characterization of the Particle Size and the Crystallinity of Certain Minerals by IR Spectrophotometry and other Instrumental Methods—II. Investigations on Quartz and Feldspar. *Clays Clay Miner.* **1978**, *26*, 139–143. [CrossRef]
42. Legodi, M.; De Waal, D. Raman spectroscopic study of ancient South African domestic clay pottery. *Spectrochim. Acta Part A Mol. Biomol. Spectrosc.* **2007**, *66*, 135–142. [CrossRef]
43. Medeghini, L.; Lottici, P.P.; De Vito, C.; Mignardi, S.; Bersani, D. Micro-Raman spectroscopy and ancient ceramics: Applications and problems. *J. Raman Spectrosc.* **2014**, *45*, 1244–1250. [CrossRef]

Disclaimer/Publisher's Note: The statements, opinions and data contained in all publications are solely those of the individual author(s) and contributor(s) and not of MDPI and/or the editor(s). MDPI and/or the editor(s) disclaim responsibility for any injury to people or property resulting from any ideas, methods, instructions or products referred to in the content.